

1 **Application of the modal superposition technique combined with**
2 **analytical elastoplastic approaches to assess the fatigue crack**
3 **initiation on structural components**

4

5 **Horas, Cláudio S.C.**

6 *CONSTRUCT-LESE, University of Porto, Faculty of Engineering, Rua Dr. Roberto Frias, 4200-*
7 *465 Porto, Portugal.*

8 *ORCID ID: 0000-0002-9868-3270*

9

10 **Correia, José A. F. O.**

11 *INEGI, University of Porto, Faculty of Engineering, Rua Dr. Roberto Frias, 4200-465 Porto,*
12 *Portugal.*

13 *ORCID ID: 0000-0002-4148-9426*

14

15 **De Jesus, Abilio M.P.**

16 *INEGI, University of Porto, Faculty of Engineering, Rua Dr. Roberto Frias, 4200-465 Porto,*
17 *Portugal.*

18 *ORCID ID: 0000-0002-1059-715X*

19

20 **Kripakaran, P.**

21 *University of Exeter, College of Engineering, Harrison building (Room 181), North Park Road,*
22 *Exeter EX4 4QF, United Kingdom*

23

24

25 **Calçada, Rui**

26 *University of Porto, Faculty of Engineering, Rua Dr. Roberto Frias, 4200-465 Porto, Portugal.*

27 *ORCID ID: 0000-0002-2375-7685*

28

29 **Corresponding author:**

30 **Horas, Cláudio S.C.**

31 University of Porto, Faculty of Engineering

32 Rua Dr. Roberto Frias, 4200-465 Porto, Portugal.

33 claudio.silva.horas@fe.up.pt

34 +351 22 508 21 87

35

36 ***Abstract***

37 Local fatigue approaches, such as, the stress-life, strain-life or energetic approaches defines a
38 framework to estimate the fatigue crack initiation from notches of structural details. Various
39 engineering structures, such as, bridges, wind towers, among others, are subjected to cyclic
40 dynamic loadings which may substantially reduce the strength of these structures. Nowadays, the
41 structural systems tend to be more complex being necessary to find computationally efficient
42 solutions to perform their fatigue analysis, accounting for dynamic actions corresponding to long
43 complex loading events (e.g. diversity of trains crossing a bridge), mainly if local approaches are
44 envisaged. Thus, this paper aims at presenting and validating a generalization of a methodology
45 based on modal superposition technique, for fatigue damage parameters evaluation, which can be
46 applied in fatigue analysis using local approaches. This technique was applied recently in the
47 context of fatigue crack propagation based on fracture mechanics, although it can be extended to
48 compute the history of local notch stresses and strains at notches. A very important conclusion is
49 that the technique can be explored for the case of local confined plasticity at notches whenever the
50 global elastic behaviour of the component prevails. Local submodelling can be explored with this
51 technique to avoid the necessity of large computational models. Local models are only needed to be
52 run under linear elastic conditions for the selected modal shapes of the structure, being the local
53 time history of fatigue damage variable computed by modal superposition for each loading event.
54 That time history may be further post-processed for elastoplastic conditions using Neuber or
55 Glinka's analyses. Comparisons with direct integration elastoplastic dynamic analysis confirmed
56 the feasibility of the proposed approach.

57 ***Keywords:*** *Fatigue local models; Modal superposition; Dynamic analysis; Cyclic elastoplastic*
58 *analysis; Structural notched components.*

59

60

61

62 **Nomenclature**

63	a	half of the crack length (crack length in the case of a lateral crack)
64	b	cyclic fatigue strength exponent
65	c	fatigue ductility exponent
66	C	geometry-dependent factor of the stress intensity factor
67	\underline{C}	damping matrix
68	D	fatigue damage
69	E	Young modulus
70	\underline{F}	nodal forces vector dependent of the dynamic load
71	f	nodal forces vector dependent of the dynamic load of the i^{th} mode of vibration
72	k_t	stress concentration factor
73	k_i	modal stiffness of the i^{th} mode of vibration
74	K	stress intensity factor
75	K'	cyclic strain hardening coefficient
76	\underline{K}	stiffness matrix
77	K_{dyn}	stress intensity factor due to the dynamic loading
78	K_i	stress intensity factor related with the i^{th} mode of vibration
79	K_{stat}	stress intensity factor due to the static loading
80	\underline{M}	mass matrix
81	m_i	modal mass of the i^{th} mode of vibration
82	n'	cyclic strain hardening exponent
83	N_f	number of cycles to the crack initiation
84	n_f	number of cycles to failure related with a certain $\Delta\sigma_{nom}$

85	p	magnitude of the loading
86	t	time
87	v	load velocity
88	Y	geometry-dependent stress intensity magnification factor
89	Y_i	modal coordinate of the i^{th} mode of vibration
90	α	Rayleigh law damping coefficient
91	β	Rayleigh law damping coefficient
92	Δt	time step increment
93	$\Delta\sigma$	local stress range
94	$\Delta\sigma_{nom}$	nominal stress range
95	$\Delta\sigma^E$	local elastic stress range
96	$\Delta\sigma^{EP}$	local elastoplastic stress range
97	$\Delta\varepsilon^E$	local elastic strain range
98	$\Delta\varepsilon^{EP}$	local elastoplastic strain range
99	$\Delta\varepsilon^p$	plastic strain range
100	$\Delta\varepsilon$	local elastoplastic strain range
101	ε'_f	fatigue ductility coefficient
102	ξ_i	damping coefficient associated to the i^{th} mode of vibration
103	ρ	material density
104	σ_{stat}	nominal static stress
105	σ_{dyn}	nominal dynamic stress
106	σ_i	modal stress related with the i^{th} mode of vibration
107	σ'_f	cyclic fatigue strength coefficient
108	σ_m	mean stress
109	ϕ_i	mode shape of the i^{th} mode of vibration

- 110 ϕ_{stat} static deformed shape
- 111 w_i natural frequency of the i^{th} mode of vibration
- 112

113 **1. Introduction**

114 The local and global collapse of large structures due to progressive fatigue damage is a problem
115 that, from a structural point of view, has been gaining importance in design, rehabilitation and
116 maintenance of these structural systems. The development of fatigue damage can be divided in two
117 different steps: firstly, a crack initiation phase takes place, which is followed by a crack propagation
118 phase that is developed until an instability condition may occur, making unsafe the operation of the
119 structure.

120 Fatigue damage can be assessed using different methods, namely global S-N approaches, local
121 stress, strain and energetic approaches and Fracture Mechanics based approaches. The global S-N
122 approach has been proposed to establish a relation between the nominal or geometric stress range
123 applied to the structural detail and the whole fatigue life of the detail, being the one that is most
124 considered in design codes, including Eurocode 3, Part 1-9 [1]. This approach has some important
125 limitations; among them the fact of being applicable only to a limited number of structural details
126 and simple loading conditions as anticipated in the codes and also not accounting for the material
127 influence since S-N curves are generally applicable for a broad range of materials. The local and the
128 Fracture Mechanics approaches can be used as more precise alternatives to the S-N methodology. In
129 fact, in the study of large metallic structures, the applicability of the local approaches has been
130 gaining importance to evaluate the fatigue issues [2–5].

131 The number of cycles required for the fatigue crack initiation may be computed using a local notch
132 approach which, considering the localized nature of the early stage fatigue damage, proposes a
133 correlation between a local parameter (e.g. strain, energy) and the required cycles to initiate a
134 macroscopic crack. The most well-known relations in this area derive from proposals by Basquin
135 [6], Coffin [7], Manson [8] and Morrow [9,10]. Very often the application of these relations requires
136 elastoplastic analyses since plasticity may develop at notch roots and their vicinities. With this
137 respect, the approximate analytical tools, such as the ones provided by the combination of the

138 Ramberg-Osgood [11], Neuber [11] and Glinka [13–15] approaches, can be applied to establish the
139 relation between the local assumed elastic stress/strain histories and the actual elastoplastic
140 stress/strain histories.

141 The Fracture Mechanics can be applied to study the fatigue crack propagation problem,
142 complementing the local approaches or allowing the calculation of the residual fatigue life of a
143 structural detail with an initial crack. This approach is supported by fatigue crack propagation laws,
144 being the Paris' law the most important one [16,17].

145 The feasibility and accuracy of the determination of the stress ranges or other local fatigue damage
146 variables, is related to the quality of the modelling. The increment of the complexity of the
147 structural system leads, naturally, to significant numerical modelling challenges which appear to be,
148 in most of the cases, associated to complex geometries and to difficulties in defining completely the
149 dynamic loading. Algorithms for solving the dynamic numerical problems, as Newmark [18] or
150 Hilber-Hughes-Taylor (HHT) [19], often require the calculation of thousands of load steps, leading
151 to a process with excessive computation time that hinders refined analyses aiming at computing the
152 local fatigue damage. Having in mind the referred limitations, it was proposed by Albuquerque et
153 al. [20,21] the modal superposition technique for the computation of stress intensity factors for a
154 propagating crack, assuming a linear global behaviour, and combining structural global and local
155 submodels, a fact that allows the global model of the structure to be simplified without neglecting
156 the correct numerical representation of the structural behaviour [2,3,22–24].

157 The crack initiation mechanisms from notches may involve the development of a localized plastic
158 zone around the stress concentrator apex. However in most practical structural applications it can be
159 said that local elastoplastic response does not interfere with the global behaviour of the structure
160 which is still expected to be linear. Also even with local crack initiation the structural system,
161 globally, behaves as linear. Such conditions should allow the application of the modal superposition

162 which can lead to significant gains in terms of computational times. Computational costs could be
163 further optimized, in the study of large structures, adopting submodelling techniques [25].
164 Considering the above mentioned, the aim of this paper is to propose the use of the modal
165 superposition technique to determine the dynamic structural response, in particular to compute the
166 notch elastoplastic stress/strain histories including the stress and strain ranges, in order to allow
167 evaluating the fatigue crack initiation phase, using the local fatigue approaches. Two different
168 routes, involving the suggested modal superposition methodology for fatigue crack initiation
169 assessment and the consideration or not of submodelling technique, are proposed. Moreover, the
170 efficiency of suggested technique is evaluated using a case study of a simple supported beam
171 submitted to dynamic load events, being the structural behaviour analysed through the proposed
172 modal superposition technique and compared with the results provided by the application of the
173 HHT algorithm [2], the latter considered as reference values.

174

175 **2. Theoretical background**

176 The theoretical background underlying to the proposed methodology in this paper, linking the
177 concepts of the modal superposition method, local approaches, either to perform elastoplastic
178 analysis or to compute the necessary number of cycles of a dynamic loading for crack initiation and
179 the possibility of using submodelling techniques is presented in this section.

180

181 **2.1. Analysis of dynamic structural behaviour using modal superposition**

182 A cyclic loading acting on a structural system gives origin to a dynamic behaviour highly dependent
183 of the characteristics of the structure and of the loading history. If this loading is known and well
184 characterized, the dynamic behaviour of the structure can be simulated using a numerical finite
185 element model, which allows computing the nodal forces for each time step. These values, related
186 to the loading on a certain time, added to the knowledge of the structural properties like mass,

187 stiffness and damping allows characterizing the structural system and its dynamic behaviour
 188 through the consideration of a direct time integration method or using the modal superposition
 189 technique. The dynamic behaviour of the structural system can be defined by the system of
 190 equations (1):

$$\underline{M} \cdot \ddot{u}(t) + \underline{C} \cdot \dot{u}(t) + \underline{K} \cdot u(t) = \underline{F}(t) \quad (1)$$

191 where \underline{M} is the mass matrix, \underline{C} the damping matrix, \underline{K} the stiffness matrix, each with a dimension of
 192 $N \times N$, \underline{F} the nodal forces vector, $N \times 1$, for a certain time step, $u(t)$, $\dot{u}(t)$ and $\ddot{u}(t)$, respectively, the
 193 vectors of displacement, velocities and acceleration whose terms are associated to the N degrees of
 194 freedom. The computation of equation (1) can be done using a direct time integration method for
 195 each time step, although it is easily understood that for structural systems with a large number of
 196 degrees of freedom the computational costs starts to be very significant or even unsustainable.

197 The modal superposition technique is computationally more efficient than the direct time
 198 integration once the global dynamic behavior of the structure can be properly reproduced
 199 considering the superposition of a limited number of vibration modes, being this possible if the
 200 structure has a global elastic behavior and has invariant properties along the time. Using the modal
 201 superposition method, the system of $N \times N$ simultaneous equations is converted in N uncoupled
 202 equations that can be solved independently [26]:

$$\ddot{Y}_i(t) + 2w_i \cdot \xi_i \cdot \dot{Y}_i(t) + w_i^2 \cdot Y_i(t) = f_i(t) \quad (2)$$

203 As already referred, equation (2) is the decoupled equation related to the vibration mode i , where
 204 $Y_i(t)$ is the modal coordinate vector, w_i the natural frequency, ξ_i the damping coefficient, and $f_i(t)$
 205 the vector of nodal forces associated to the N degrees of freedom for the vibration mode i . Besides
 206 the decoupling of the vibration modes, and subsequent transformation of the N simultaneous
 207 equations system into i decoupled equations, the efficiency of the modal superposition is further

208 increased by the fact of the number of modes being in general much smaller than the number N of
 209 the degrees of freedom.

210 Albuquerque *et al.* [20,21] proposed the use of modal superposition technique to study the dynamic
 211 behavior of a structure with an initial elliptical crack aiming at computing the stress intensity factor
 212 histories, $K(t)$, being such information essential to predict the fatigue crack propagation through
 213 fatigue crack propagation laws, such as the Paris' law. The stress intensity factor can be computed
 214 by the following equation:

$$K(t) = C \cdot \sigma(t) \cdot \sqrt{\pi a} \quad (3)$$

215 where C is a parameter that depends on the geometry of the structure and on the crack dimensions,
 216 $\sigma(t)$ is the nominal stress history acting on the detail and a the crack dimension. Taking into
 217 account that the loading acting on a structure can be composed by static and dynamic components,
 218 the stress intensity factor can result from the sum of two different values, K_{stat} and $K_{dyn}(t)$, one
 219 that depends on the static stress level, σ_{stat} , and another that depends on the dynamic stress,
 220 $\sigma_{dyn}(t)$:

$$K(t) = K_{stat} + K_{dyn}(t) \quad (4)$$

$$K_{stat} = C \cdot \sigma_{stat} \cdot \sqrt{\pi a} \quad (5)$$

$$K_{dyn}(t) = C \cdot \sigma_{dyn}(t) \cdot \sqrt{\pi a} \quad (6)$$

221 As already referred, the modal superposition method can be applied to structures with a global
 222 linear behavior which means that it is only applicable to assess the crack initiation or crack
 223 propagation due to fatigue when the local plasticity phenomenon or the non-linear contact between
 224 crack faces do not influence the linearity of global behavior. Thus, if these assumptions are verified,
 225 the dynamic stress can be determined by:

$$\sigma_{dyn}(t) = \sum_i \sigma_i \cdot Y_i(t) \quad (7)$$

226 where σ_i is the nominal stress associated to the i^{th} mode shape and $Y_i(t)$ is, as already referred, the
 227 modal coordinate of the i^{th} mode of vibration. Considering equations (6) and (7), the determination
 228 of the stress intensity factor is performed according to:

$$K_{dyn}(t) = C \cdot \sum_i \sigma_i \cdot Y_i(t) \cdot \sqrt{\pi a} = \sum_i K_i \cdot Y_i(t) \quad (8)$$

229 K_i can be defined as the stress intensity factor obtained for the mode shape of the i^{th} mode of
 230 vibration, which means the modal stress intensity factor. Thus, the total stress intensity factor can
 231 be computed by:

$$K(t) = K_{stat} + \sum_i K_i \cdot Y_i(t) \quad (9)$$

232 The logic underlying the concept of the modal stress intensity factors can be extended to other local
 233 structural quantities as stresses, strains or energetic parameters. Thus equations (4) and (8) can be
 234 written in the following general form:

$$\psi(t) = \psi_{stat} + \sum_i \psi_i \cdot Y_i(t) \quad (10)$$

235 where ψ can be a generic fatigue damage quantity (e.g. stress, strain, energy, stress intensity, J-
 236 Integral, COD), being ψ_{stat} the part of this quantity that depends on the static loading and ψ_i the
 237 modal value determined considering the mode shape of the i^{th} mode of vibration. Taking into
 238 account equation (10) it is easily understandable that the modal superposition can be extended to
 239 compute local quantities required to assess the crack initiation due to fatigue phenomenon.

240

241 **2.2. Crack initiation assessment**

242 The fatigue crack initiation can be analyzed considering local approaches which require the
 243 computation of local fatigue damage parameters in order to establish a relation between these local
 244 parameters and the number of cycles required to the crack initiation. The most well-known relations
 245 in this area are the Basquin [6], equation (11), Coffin [7] and Manson [8], equation (12), Basquin-
 246 Coffin-Manson [5], equation (13), and Morrow [10], equation (14):

$$\frac{\Delta\sigma}{2} = \sigma_f'(2N_f)^b \quad (11)$$

$$\frac{\Delta\varepsilon^P}{2} = \varepsilon_f'(2N_f)^c \quad (12)$$

$$\frac{\Delta\varepsilon^{EP}}{2} = \frac{\sigma_f'}{E}(2N_f)^b + \varepsilon_f'(2N_f)^c \quad (13)$$

$$\frac{\Delta\varepsilon^{EP}}{2} = \frac{\sigma_f' - \sigma_m}{E}(2N_f)^b + \varepsilon_f'(2N_f)^c \quad (14)$$

247 where $\Delta\sigma$ is the local stress range, $\Delta\varepsilon^P$ the plastic stress range, $\Delta\varepsilon^{EP}$ the local elastoplastic strain
 248 range, σ_f' and b , respectively, the cyclic fatigue strength coefficient and exponent, ε_f' and c ,
 249 respectively, the fatigue ductility coefficient and exponent, σ_m the mean stress, N_f the number of
 250 cycles to the crack initiation, and E the Young modulus. Taking into account these quantities, and in
 251 order to use the stress/strain results after a linear elastic finite element analysis, a relation between
 252 the nominal elastic stress and the local notch elastoplastic stress/strain range can be established
 253 using the Neuber [12], equation (15), or Glinka [13–15], equation (16), and the Ramberg-Osgood
 254 [11], equation (17), relations.

$$\frac{(k_t \Delta\sigma_{nom})^2}{E} = \frac{\Delta\sigma^2}{E} + 2\Delta\sigma \left(\frac{\Delta\sigma}{2K'}\right)^{1/n'} \quad (15)$$

$$\frac{(k_t \Delta\sigma_{nom})^2}{E} = \frac{\Delta\sigma^2}{E} + \frac{4\Delta\sigma}{n'+1} \left(\frac{\Delta\sigma}{2K'}\right)^{1/n'} \quad (16)$$

$$\Delta\varepsilon = \frac{\Delta\sigma}{E} + 2 \left(\frac{\Delta\sigma}{2K'}\right)^{1/n'} \quad (17)$$

255 In equations (15)-(17), k_t is the elastic stress concentration factor, K' are n' are, respectively, the
 256 cyclic strain hardening coefficient and exponent and $\Delta\sigma_{nom}$ the nominal elastic stress range,
 257 computed near the notch. Analyzing the expressions presented above, equations (11)-(17), it is clear
 258 that besides the material constants/parameters, k_t and $\Delta\sigma_{nom}$ are the only unknowns. If the value of
 259 k_t can be eventually determined through a static analysis using the finite element model, the
 260 nominal stress range can only be obtained after the dynamic analysis of the structural system, which

261 means that $\Delta\sigma_{nom}$ can be computed solving equation (1) applying a direct time integration method
 262 or, more efficiently, the modal superposition technique.

263 In the case of complex structures, the elastic stress concentration factor, k_t , is not easy to compute
 264 since the definition of the nominal stress is generally not clear. The application of the Neuber [12]
 265 and Glinka [13-15] approaches need to be performed without the stress concentration factor
 266 formulation, relating directly the local elastic stress/strain field with the local elastoplastic
 267 stress/strain field:

$$\Delta\sigma^E \cdot \Delta\varepsilon^E = \frac{\Delta\sigma^{EP^2}}{E} + 2\Delta\sigma^{EP} \left(\frac{\Delta\sigma^{EP}}{2K'} \right)^{1/n'} \quad (18)$$

$$\Delta\sigma^E \cdot \Delta\varepsilon^E = \frac{\Delta\sigma^{EP^2}}{E} + \frac{4\Delta\sigma^{EP}}{n'+1} \left(\frac{\Delta\sigma^{EP}}{2K'} \right)^{1/n'} \quad (19)$$

268 where $\Delta\sigma^E$ and $\Delta\varepsilon^E$ are, respectively, the local elastic stress and strain ranges at the notch, and
 269 $\Delta\sigma^{EP}$ and $\Delta\varepsilon^{EP}$ the local elastoplastic stress and strain ranges at the same point. In simple cases the
 270 value of $\Delta\sigma^E$ is indirectly calculated through $k_t \cdot \Delta\sigma_{nom}$, something that is not expected when the
 271 structural geometry and loading are complex. Also, in the simpler version of Neuber/Glinka
 272 relations $\Delta\varepsilon^E$ is computed from $\Delta\sigma^E/E$ but this is an approximation only valid for near uniaxial
 273 stress conditions. For multiaxial stress states, the numerical model will provide a better
 274 approximation for the elastic strain and consequently the energy term, $\Delta\sigma^E \cdot \Delta\varepsilon^E$.

275

276 **2.3. Submodelling**

277 Generally, the global numerical model of a large structure, even when built with beam or shell
 278 elements discretized with a coarse mesh, is able to properly reproduce the dynamic global
 279 behaviour [2,3,24]. However, despite the accuracy of these results, a local fatigue analysis demands
 280 a much more refined model, typically built with shell or brick elements, which tend to be hard to
 281 handle using a global model because it increases significantly the computational costs.

282 An alternative approach, lighter in terms of computational costs, consists in the analysis of the
 283 global model and the subsequent imposition of the obtained displacement field to a refined local
 284 model. Hence, the utilization of submodelling techniques, such as beam-to-shell, shell-to-shell,
 285 shell-to-solid, beam-to-solid, are particularly useful since the displacement fields from the global
 286 model is applied to the local model using shape functions which means that there are not any
 287 constraints to the global or local modelling.

288

289 **2.4. Computational algorithm**

290 Considering the main objectives of this paper, the simulation of fatigue crack initiation using local
 291 approaches and the modal superposition method to assess the local damage parameters, the
 292 following steps are proposed:

- 293 • Computation of nominal stress, σ_{stat} , and displacement field, ϕ_{stat} , due to the static loading;
- 294 • Modal analysis of the structure and consequent calculation, for each i^{th} vibration mode, of the
 295 modal frequencies, w_i , the modal mass, m_i , the modal stiffness, k_i , and the vibration mode
 296 shapes, Φ_i ;
- 297 • Evaluation of the dynamic loading, $F(t)$, and determination of the nodal forces, $f_i(t)$;
- 298 • Calculation of the time histories of the modal coordinates, $Y_i(t)$;
- 299 • Computation of the nominal stress spectrum, $\sigma_{nom}(t)$, considering the static and dynamic parts:

$$\sigma_{nom}(t) = \sigma_{stat} + \sum_i \sigma_i \cdot Y_i(t) \quad (20)$$

- 300 • Determination of the mean stress, σ_m ;
- 301 • Selection of the local approach depending on whether the detail remains elastic or not;
- 302 • Calculation of the nominal stress range, $\Delta\sigma_{nom}$, and the corresponding number of cycles, n_f ,
 303 applying the rainflow method to the nominal stress spectrum, $\sigma_{nom}(t)$;
- 304 • Determination of the required number of cycles to the crack initiation, N_f , applying a local
 305 approach;

306 • Computation of the linear accumulation damage, D , using the Miner's relation:

$$D = \sum \frac{n_f}{N_f} \tag{21}$$

307 Taking into account the presented computational algorithm, the steps sequence to assess the
 308 necessary number of cycles to the crack initiation can be summarized as shown in Fig. 1. The
 309 computational algorithm may include, or not, the consideration of the submodeling techniques. If it
 310 is not considered a submodel, the nominal stress spectrum is computed after the application of the
 311 modal superposition method to the global model (Fig. 2).

312 The proposed methodology, besides the already referred advantages, presents a major value in
 313 terms of the computation process when several calculations related with different loading scenarios
 314 are needed. More specifically, for each time step, the consideration of several dynamic events only
 315 requires the definition of $f_i(t)$ and $Y_i(t)$ for each loading and not the solution of the $N \times N$ system of
 316 simultaneous equations for each dynamic event.

317

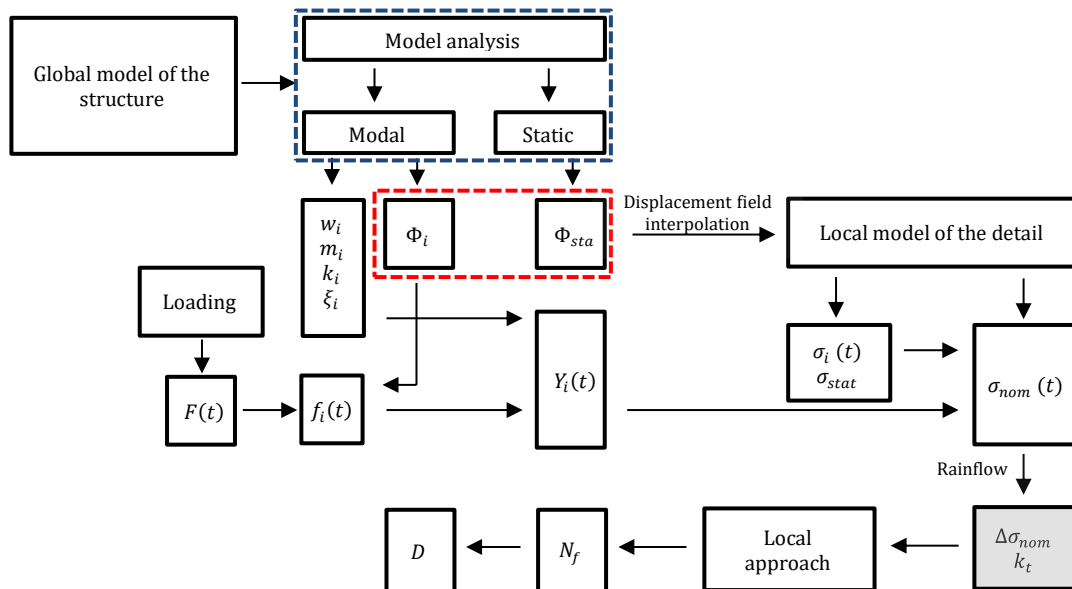


Fig. 1. Flow chart for the application of the proposed modal superposition methodology for fatigue crack initiation assessment (with submodeling).

318

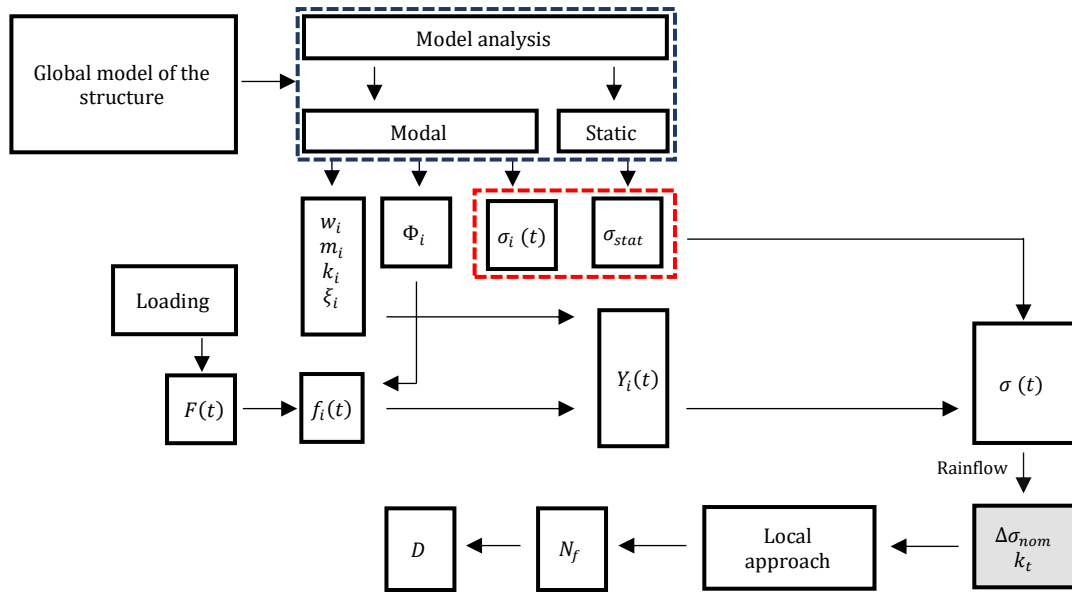


Fig. 2. Flow chart for the application of the proposed modal superposition methodology for fatigue crack initiation assessment (without submodeling).

319

320 For both of the presented computational algorithms pictured in the Fig. 1 and Fig. 2 it is necessary
 321 to know in advance the elastic stress concentration factor. If the structural engineer has to deal with
 322 a complex structure, as already mentioned, the value of k_t is not easily computed, being necessary
 323 working directly with the elastic notch stress/strains, σ^E and ε^E from the FE analysis. Also, after
 324 computing the local/notch elastic stress/strain histories, one may apply the Neuber or Glinka
 325 analyses to derive the local elastoplastic stress/strain histories, the fatigue cycles resulting directly
 326 from hysteresis loops counting and not from the rainflow analysis. Hysteresis cycles counting is
 327 more consistent with fatigue damage.

328 The proposed modal superposition technique for the computation of local fatigue damage
 329 parameters was explored in previous works concerning the application of Fracture Mechanics
 330 principles to the fatigue crack propagation analysis [2,3,20,21]. In the present paper a generalization
 331 and complementary approach is proposed for the computation of fatigue damage parameters aiming
 332 at simulating fatigue crack initiation. In both cases, crack closure effects (Fracture Mechanics) and
 333 local notch elastoplasticity (fatigue crack initiation) are expected non-linearities, but while they do
 334 not change the global linear behaviour of the structure, the modal superposition can be successfully

335 applied. For large structures the fatigue crack initiation process does not influence the global
336 behaviour of the structure, therefore modal analysis only needs to be performed one time. However,
337 when fatigue crack propagation is performed, it is worthwhile to refer that the propagating fatigue
338 crack may change the global behaviour of the structure which may require periodic updates of the
339 structural vibration modes.

340

341 **3. Crack initiation assessment – application to a notched structural member**

342 In order to validate the applicability of the modal superposition methodology for fatigue crack
343 initiation assessment, a numerical model of a notched simple structure was developed and duly
344 characterized from a geometric and material point of view. According to the computational
345 algorithm presented in the section 2.4, the flow chart pictured in Fig. 2 was implemented, i.e., the
346 explicit submodelling was not applied. The option for a simple structure was taken in order to
347 control all the parameters with direct or indirect influence in the structural dynamic behaviour.

348 The effectiveness of the proposed methodology is naturally dependent on the analytical
349 elastoplastic approach considered, hence the referred influence was tested through the consideration
350 of the Neuber [12] and Glinka [13-15] proposals. Instead of $k_t\sigma_{nom}$ based elastoplastic
351 formulations, elastoplastic analyses formulated from the local elastic stress/strain computed directly
352 from the finite element model, Equations (18)-(19), are used.

353 The finite element model was submitted to dynamic loadings with variable intensity obtained
354 through the moving loads approach. The dynamic analyses were carried out using the proposed
355 modal superposition methodology with post-processing elastoplastic analysis and HHT algorithm
356 [18] coupled with elastoplastic material behaviour, being compared the obtained stress-strain
357 diagrams. Additionally, the necessary number of cycles to the crack initiation, N_f , is computed
358 using the Morrow approach [10]. The extension of local plastic volume is also evaluated and
359 commented as regards the reliability of the simulated modal superposition methodology.

360

361 **3.1. Structure description**

362 A notched simply supported steel beam, with a 10m span and a HEB 700 cross section was
 363 idealised. At mid span a circular hole with 10mm of radius was admitted to simulate a notch/defect
 364 on the inferior flange. The numerical model was conceived using the ANSYS software [27] (Fig.
 365 3).

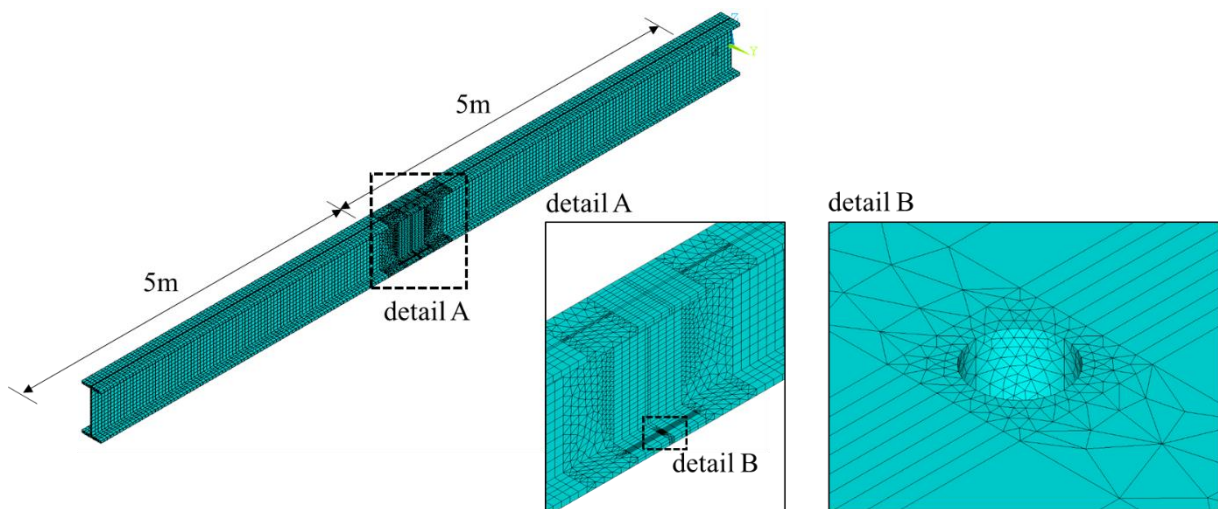


Fig. 3. Finite element model of a simple supported beam with a circular hole at the lower flange.

366

367 The finite element model was built with 20-node brick elements with mesh refinement on the
 368 notched zone to improve the description of the local stress and strain fields [28]. The beam is
 369 assumed of S355 steel which was characterized in terms of elastoplastic behaviour and fatigue by
 370 De Jesus et al. [29]. In the HHT analysis, the material is assumed elastoplastic in a central length of
 371 4m of the bottom flange and web. The remaining of the structure was assumed linear elastic with
 372 the same density (ρ), Young modulus (E) and Poisson ratio (ν) of the elastoplastic material. These
 373 two materials option corresponds to a partial submodelling that helps numerical convergence and
 374 computation costs reduction. Fig. 4 represents the elastoplastic stress-strain cyclic curve of the S355
 375 steel grade, adapted from De Jesus et al. [29].

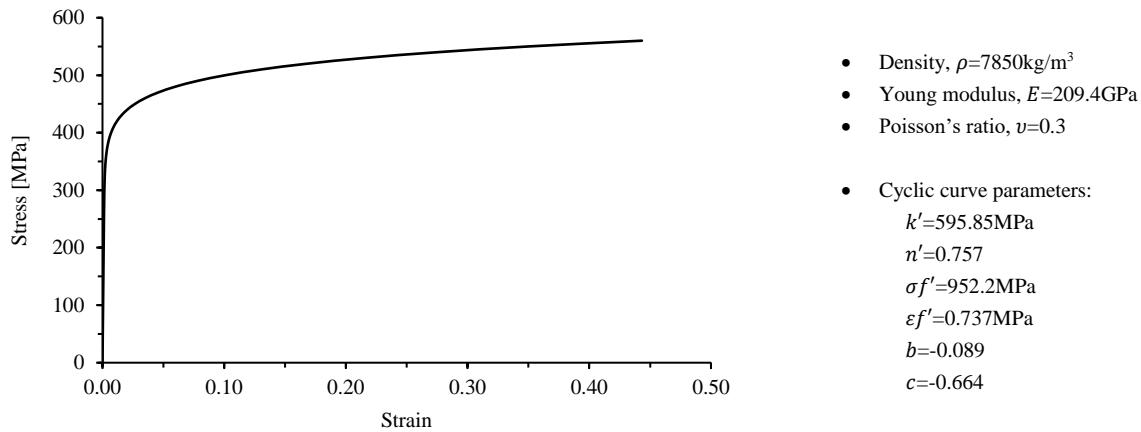


Fig. 4. Cyclic stress-strain curve of the S355 grade (adapted from [29]).

376

377 In Fig. 4., the material parameters required to perform a cyclic elastoplastic analysis taking into
 378 account the Neuber [12], Eqs. (15) or (18), or Glinka [13-15], Eqs. (16) or (19), approaches and,
 379 subsequently, to compute the necessary number of cycles to the crack initiation, N_f , according to
 380 Morrow [10], eq. (14), are presented.

381

382 3.2. Dynamic analysis assumptions

383 The structural mass was calibrated in order the main natural frequencies being close to available
 384 data in the literature [30], seeking to approximate the idealized structure of a practical case. The
 385 stiffness was determined for the described simple supported beam considering the defined cross
 386 section, although it should be noted that the out of plane degrees of freedom were also restrained in
 387 order to eliminate purely local modes, without contributions to the global dynamic behavior, and
 388 whose existence is only possible due to the absence of transverse bracing.

389 In the modal superposition analysis, a constant modal damping ratio, ξ , of 0.5% was assumed for all
 390 the considered modes; concerning the calculation considering the HHT algorithm [19] it was
 391 assumed a Rayleigh damping law characterized with the coefficients α equal to 0.682414 and β to
 392 0.000024, values computed considering the first and third modes of vibration [26]. In the analyses,

393 a time step increment, Δt , equal to 0.0001s and a residual free vibration period of 0.1s were
 394 admitted.

395 Taking into account the simplicity of the structure, it was expected a small number of modes to
 396 contributed significantly to the total dynamic response. A sensitivity analysis allowed to prove such
 397 assumption, being considered only the first 5 vibration modes to capture accurately the total
 398 structural response.

399

400 **3.3. Dynamic loading**

401 Several dynamic loadings were considered to evaluate the efficiency of the proposed methodology
 402 and the influence of the plasticity phenomenon at the notched bottom flange. In a given time
 403 instant, t , the nodal loads were computed with base on their position along the beam and on the
 404 node coordinates. Each loading, characterized by a given magnitude, p , and by a certain velocity, v ,
 405 applies only one cycle to the structure, n_f . The considered dynamic loads are summarized in Table
 406 1.

407

Table 1. Considered dynamic loading: moving concentrated loadings.

Loading Id	(1)	(2)	(3)	(4)	(5)	(6)
p (kN)	800	800	900	900	1000	1000
v (km/h)	100	200	100	200	100	200

408

409 As shown in Table 1, six different loadings were admitted which gave origin to eighteen dynamic
 410 analyses. Twelve performed according the proposed modal superposition methodology, six
 411 considering the Neuber approach [12], eq. (15) or (18), and other six the one proposed by Glinka
 412 [13-15], eq. (16) or (19), according to the flow chart presented in Fig. 2, and the last six applying
 413 the HHT algorithm [18] in order to allow a validation process. To avoid local singularities or
 414 unexpected resonant effects that would cause problems to the numerical convergence of the results,
 415 the loading of the structure was made considering linear loads, perpendicular to the longitudinal

416 direction of the beam, with 0.085m of development. The resultants of the linear loads were equal to
 417 the magnitude, p .

418 The implementation of the Neuber and Glinka approaches were made using the *Fatigue Life*
 419 *Prediction* –FLP software developed by Silva [31].

420

421 **3.4. Results of the dynamic analysis**

422 Taking into account the established fundamentals, the aimed dynamic analyses were carried out.

423 According to the eq. (10) the generic fatigue damage quantity, ψ , was defined as stresses and strains

424 along the longitudinal direction, allowing to obtain the stress-strains diagrams at the notch apex.

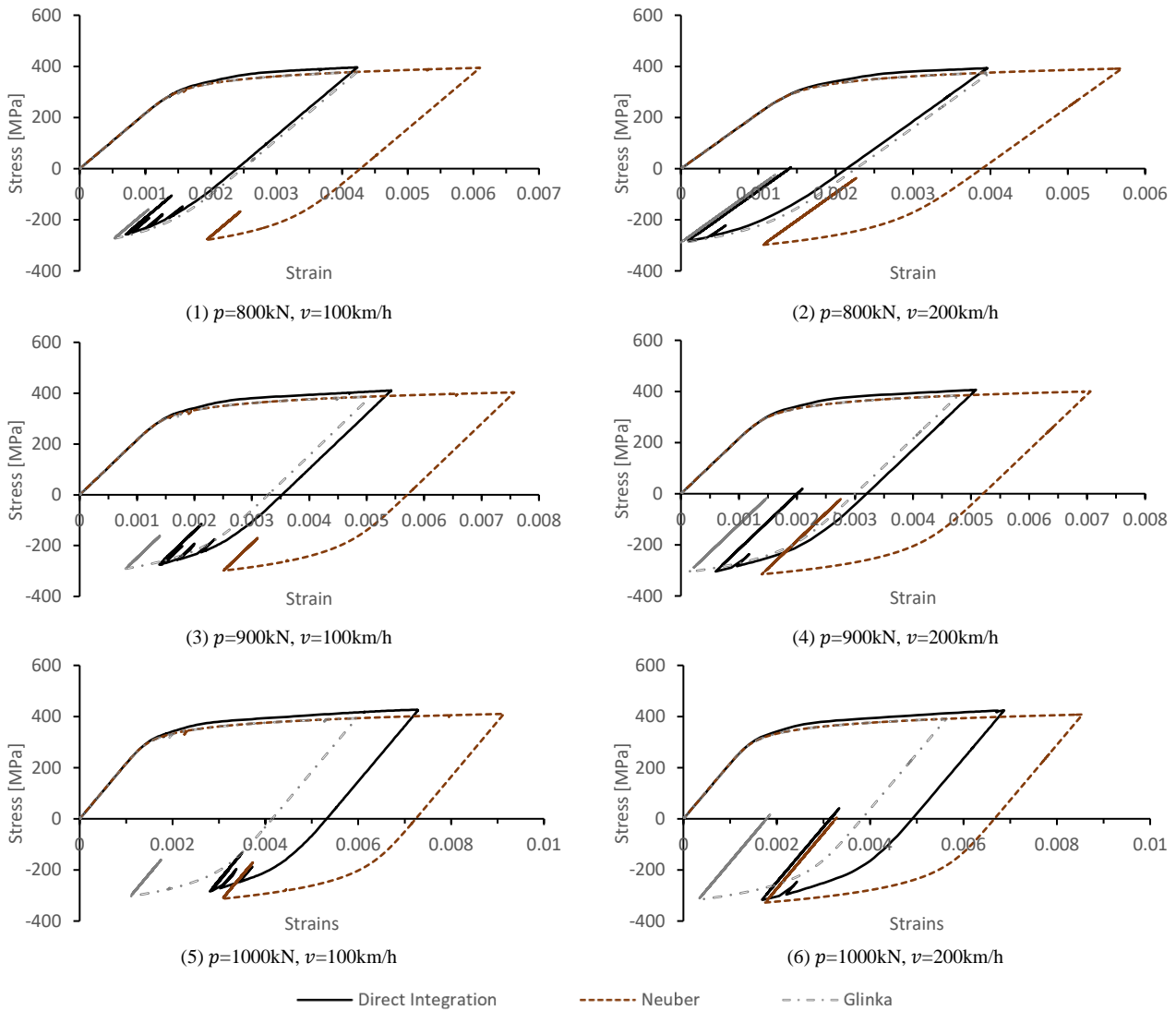


Fig. 5. Elastoplastic stress-strain diagrams under dynamic loading.

425

426 In Fig.5, it is possible to observe, for the loadings (1), (2), (3) and (4), a notorious agreement
427 between the obtained stress-strain diagrams through the modal superposition combined with the
428 Glinka approach [13-15] and the results of the direct time integrations using the HHT algorithm
429 [19]. A discrepancy between the results was found when the modal superposition was use together
430 with the Neuber approach [12], the Neuber approach resulting in higher average strains which is
431 consistent with the conservatism usually associated to this rule. Therefore, despite the plasticity
432 phenomenon, it was possible for the referred loadings to achieve satisfactory agreement in the
433 stress-strain diagrams with the modal superposition analysis plus Glinka approach. In the cases of
434 the loadings (5) and (6), the increment on the magnitude, p , resulted in the development of larger
435 plastic zones, which explain the progressive discrepancy between the stress-strain diagrams from
436 the two dynamic analyses.

437 Table 2 presents the relevant results obtained after the two dynamic analyses, including cycles
438 information in terms of strains and stresses and life estimations using the Morrow model, eq. (14).
439 Percentage differences relative to the results obtained with the HHT algorithm [19], assumed as
440 reference, (actual value/reference value-1), are also presented. The data from the table confirms the
441 conclusions pointed out after the observation of Fig. 5. The necessary number of cycles for the
442 crack initiation computed using the Morrow approach, confirmed the Neuber proposal as
443 considerably conservative. Also the deviations in the stress computations are significantly lower
444 than in strain computations. The computations of the stress and strain variations are also much more
445 precise than the minimum and maximum stress and strain values. These two considerations led to
446 accurate life predictions using the modal superposition analysis plus simplified analytical
447 elastoplastic analysis, with maximum deviations of 21% using the Glinka approach for the loading
448 (5), which is the loading generating the highest residual plastic zone (see Fig. 6). While Neuber
449 approach generated maximum deviations of 3% on stress ranges and 35% on strain ranges, the
450 Glinka approach generated deviations of -4.4% on stress range and 8.5% on stress range.

451

452

453

Table 2. Relevant results of the dynamic and fatigue analysis.

Loading	#	σ_{max} (MPa)	σ_{min} (MPa)	σ_m (MPa)	$\Delta\sigma$ (MPa)	ε_{max}	ε_{min}	ε_m	$\Delta\varepsilon$	N_f
p=800kN v=100km/h	HHT	396.25	-257.27	69.49	653.52	0.00423	0.00070	0.00247	0.00353	57953
	Neuber	394.31	-278.84	57.73	673.15	0.00610	0.00193	0.00402	0.00417	34387
	$\Delta\%$	-0.5%	8.4%	-16.9%	3.0%	44.2%	175.7%	62.8%	18.1%	-40.7%
	Glinka	378.36	-273.66	52.35	652.02	0.00423	0.00052	0.00238	0.00371	48937
	$\Delta\%$	-4.5%	6.4%	-24.7%	-0.2%	0.0%	-25.7%	-3.6%	5.1%	-15.6%
	<hr/>									
p=800kN v=200km/h	HHT	392.94	-282.37	55.28	675.31	0.00396	0.00010	0.00203	0.00387	39407
	Neuber	391.47	-298.11	46.68	689.58	0.00570	0.00106	0.00338	0.00464	21457
	$\Delta\%$	-0.4%	5.6%	-15.6%	2.1%	43.9%	960.0%	66.5%	19.9%	-45.6%
	Glinka	375.70	-290.74	42.48	666.45	0.00400	-0.00001	0.00199	0.00401	35144
	$\Delta\%$	-4.4%	3.0%	-23.2%	-1.3%	1.0%	-110.0%	-2.0%	3.6%	-10.8%
	<hr/>									
p=900kN v=100km/h	HHT	410.45	-274.78	67.83	685.23	0.00543	0.00139	0.00341	0.00404	30661
	Neuber	402.99	-298.41	52.29	701.39	0.00757	0.00251	0.00504	0.00506	15250
	$\Delta\%$	-1.8%	8.6%	-22.9%	2.4%	39.4%	80.6%	47.8%	25.2%	-50.3%
	Glinka	386.47	-290.44	48.01	676.91	0.00507	0.00080	0.00294	0.00427	26074
	$\Delta\%$	-5.8%	5.7%	-29.2%	-1.2%	-6.6%	-42.4%	-13.8%	5.7%	-15.0%
	<hr/>									
p=800kN v=200km/h	HHT	406.20	-304.26	50.97	710.45	0.00508	0.00060	0.00284	0.00448	21022
	Neuber	400.21	-315.06	42.57	715.27	0.00706	0.00139	0.00423	0.00566	10208
	$\Delta\%$	-1.5%	3.5%	-16.5%	0.7%	39.0%	131.7%	48.9%	26.3%	-51.4%
	Glinka	383.88	-305.45	39.21	689.33	0.00478	0.00014	0.00246	0.00463	19169
	$\Delta\%$	-5.5%	0.4%	-23.1%	-3.0%	-5.9%	-76.7%	-13.4%	3.3%	-8.8%
	<hr/>									
p=1000kN v=100km/h	HHT	426.93	-284.07	71.43	711.00	0.00729	0.00280	0.00504	0.00449	19658
	Neuber	410.32	-312.74	48.79	723.05	0.00914	0.00308	0.00611	0.00606	8157
	$\Delta\%$	-3.9%	10.1%	-31.7%	1.7%	25.4%	10.0%	21.2%	35.0%	-58.5%
	Glinka	393.38	-302.97	45.20	696.35	0.00597	0.00109	0.00353	0.00487	15531
	$\Delta\%$	-7.9%	6.7%	-36.7%	-2.1%	-18.1%	-61.1%	-30.0%	8.5%	-21.0%
	<hr/>									
p=1000kN v=200km/h	HHT	423.84	-316.37	53.73	740.21	0.00687	0.00168	0.00428	0.00519	12114
	Neuber	407.75	-327.64	40.05	735.40	0.00855	0.00175	0.00515	0.00680	5735
	$\Delta\%$	-3.8%	3.6%	-25.5%	-0.6%	24.5%	4.2%	20.3%	31.0%	-52.7%
	Glinka	390.96	-316.60	37.18	707.56	0.00563	0.00032	0.00297	0.00531	11650
	$\Delta\%$	-7.8%	0.1%	-30.8%	-4.4%	-18.0%	-81.0%	-30.6%	2.3%	-3.8%

454

455

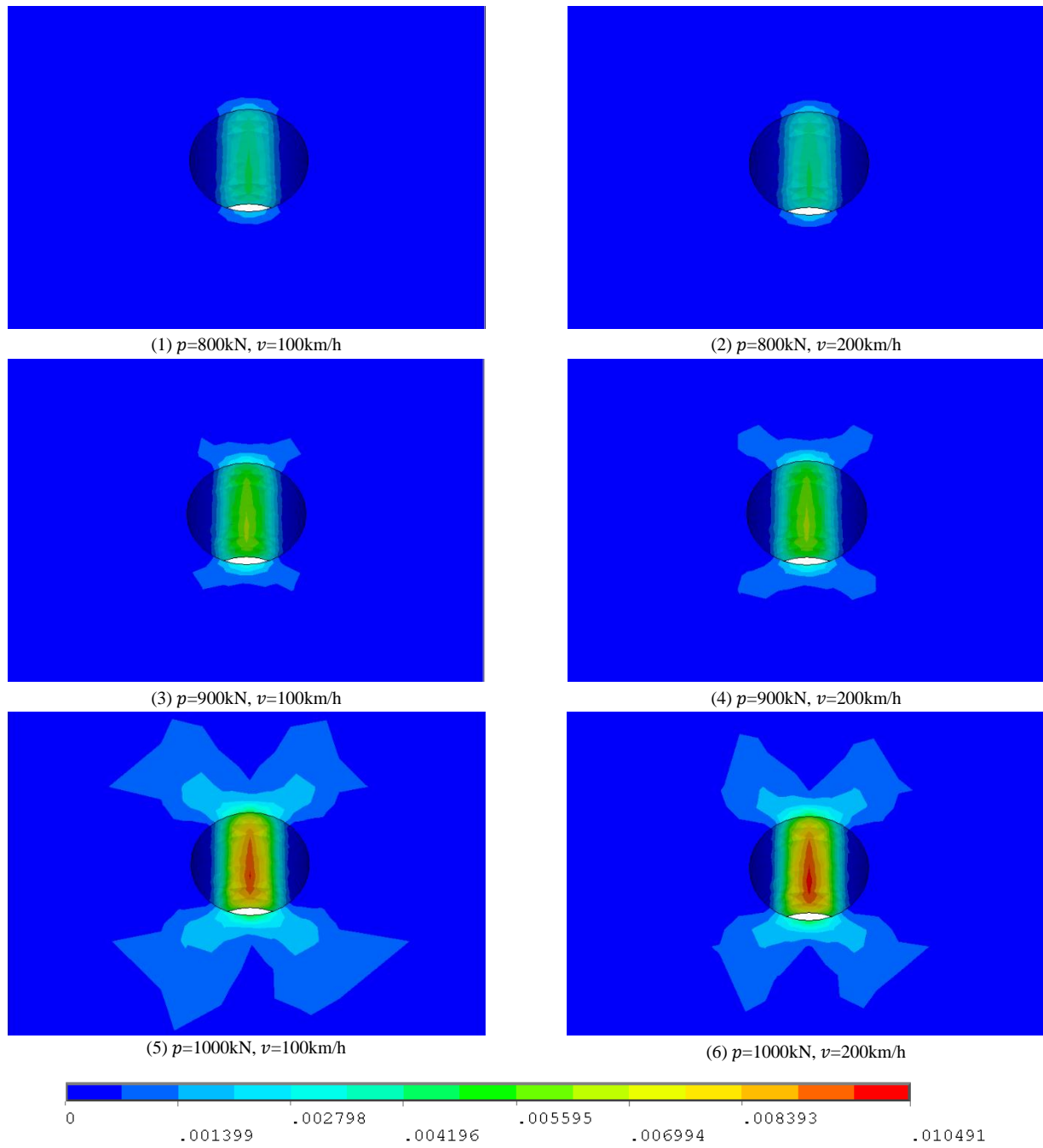


Fig. 6. Residual equivalent plastic strain, evolution of the local plastic material volume.

456

457 Fig. 6 shows the residual equivalent plastic strain fields [32] after the load passage which gives a
 458 measure of the volume of material plastically deformed. The evolution of the plastic zone with the
 459 magnitude, p , of the loading is notorious, but less important when the loading speed doubles.
 460 Nevertheless for all cases the plastic zone region is still confined and therefore no significant effect
 461 on stress and strain ranges is verified as well as in the life calculations.

462

463 **4. Concluding remarks**

464 The fatigue damage is a structural problem that is fundamental to assess in order to extend the
465 operational life of the existing structures. The scale of large structures puts significant problems in
466 terms of numerical modelling and structural analysis, particularly in what refers to the application
467 of local models to fatigue.

468 The obtained results, after the validation of the proposed modal superposition technique for fatigue
469 crack initiation assessment, allow concluding that they are promising for the analysis of more
470 complex structural problems. The proposed technique presented in the present paper, under the
471 condition of localized plasticity, combined with the work of Albuquerque *et al.* [20,21] enables the
472 structural engineer to fully assess the fatigue phenomenon using the modal superposition method.

473 The consideration of the approached technique permits to optimize the calculation process, making
474 possible the dynamic structural analysis in an affordable computational time. Regarding the simple
475 structure idealized and considering the assumption underlying the dynamic analysis, the calculation
476 involving the proposed technique took 10 seconds to compute the stress and strain results, while the
477 application of the HHT algorithm spent more than 5 hours, such difference giving a clear
478 quantification of the potential of the proposed technique. Moreover, the use of this method
479 conjugated with submodelling techniques can increase the accuracy and efficiency of refined
480 analysis of complex notched details, which means the computation of the local stress and strain data
481 required to assess the fatigue crack initiation at notches. The modal superposition analysis with the
482 Glinka elastoplastic post-processing is more precise than using the Neuber post-processing.

483 Further studies for more complex structures are needed, in particularly, the evaluation of the
484 accuracy of the results when contact non-linearities are present at the notched area (e.g. riveted
485 joints).

486

487 **Acknowledgments**

488 Authors acknowledge the Portuguese Foundation for Science and Technology for the funding,
489 particularly through the iRail doctoral program and the grants PD/BD/114101/2015 and
490 SFRH/BPD/107825/2015. Authors gratefully acknowledge the funding of SciTech - Science and
491 Technology for Competitive and Sustainable Industries (NORTE-01-0145-FEDER-000022), R&D
492 project co-financed by Programa Operacional Regional do Norte.

493

494 **References**

- 495 [1] CEN, Eurocode 3: Design of steel structures - Part 1-9: fatigue strength of steel structures,
496 (2005).
- 497 [2] C. Albuquerque, Advanced Methodologies for the Assessment of the Fatigue Behaviour of
498 Railway Bridges, Phd Thesis, Faculty of Engineering of the University of Porto, 2015.
- 499 [3] A.L.L. Silva, Advanced Methodologies for the Fatigue Analysis of Representative Details of
500 Metallic Bridges, Phd Thesis, Faculty of Engineering of the University of Porto, 2015.
- 501 [4] R.M. Teixeira, Metodologias para Modelagem e Análise da Fadiga em Ligações Rebitadas
502 com Aplicação em Pontes Metálicas Ferroviárias, Phd Thesis, Escola Politécnica da
503 Universidade de São Paulo, 2015.
- 504 [5] D. Radaj, C.M. Sonsino, W. Fricke, Fatigue Assessment of Welded Joints by Local
505 Approaches, Woodhead publishing, 2006.
- 506 [6] O.H. Basquin, The Exponential Law of Endurance Tests, Am. Soc. Test. Mater. Proc. Vol.
507 10 (1910) 625–630.
- 508 [7] L.F. Coffin, A Study of the Effects of the Cyclic Thermal Stresses on a Ductile metal, Trans.
509 ASME. Vol. 76 (1954) 931–950.
- 510 [8] S.S. Manson, Behaviour of Materials under Conditions of Thermal Stress, NACA, USA,
511 1954.

- 512 [9] J. Morrow, Cyclic Plastic Strain Energy and Fatigue of Metals, in: Intern. Frict. Damping,
513 Cycl. Plast., ASTM International, 1965: pp. 45–87. doi:10.1520/STP43764S.
- 514 [10] J. Morrow, Fatigue design handbook, in: Fatigue Prop. Met., No. AE-4, Society of
515 Automotive Engineers, Warrendale, PA., 1968: pp. 21–29.
- 516 [11] W. Ramberg, W.R. Osgood, Description of stress-strain curves by three parameters, (1943).
- 517 [12] H. Neuber, Theory of stress concentration for shear-strained prismatical bodies with arbitrary
518 nonlinear stress-strain law, J. Appl. Mech. 28 (1961) 544–550.
- 519 [13] G. Glinka, Energy density approach to calculation of inelastic strain-stress near notches and
520 cracks, Eng. Fract. Mech. 22 (1985) 485–508. doi:http://dx.doi.org/10.1016/0013-
521 7944(85)90148-1.
- 522 [14] G. Glinka, Calculation of inelastic notch-tip strain-stress histories under cyclic loading, Eng.
523 Fract. Mech. 22 (1985) 839–854. doi:http://dx.doi.org/10.1016/0013-7944(85)90112-2.
- 524 [15] G. Glinka, Relations Between the Strain Energy Density Distribution and Elastic-Plastic
525 Stress-Strain Fields Near Cracks and Notches and Fatigue Life Calculation, ASTM STP 942.
526 (1988) 1022–1047. doi:10.1520/STP24538S.
- 527 [16] D. Broek, Elementary Engineering Fracture Mechanics, 3rd ed., Martinus Nijhoff Publishers,
528 The Hague, Netherlands, 1982.
- 529 [17] C.A.G. de M. Branco, A.A. Fernandes, P.M.S.T. de Castro, Fadiga de Estruturas Soldadas, 2^a
530 ed, Fundação Calouste Gulbenkian, Lisboa, 1999.
- 531 [18] K.-J. Bathe, Finite Element Procedures, Prentice Hall Inc, New Jersey, 1996.
- 532 [19] J. Chung, G.M. Hulbert, A time integration algorithm for structural dynamics with improved
533 numerical dissipation: the generalized- α method, J. Appl. Mech. 60 (1993) 371–375.
- 534 [20] C. Albuquerque, P.M.S.T. de Castro, R. Calçada, Efficient crack analysis of dynamically
535 loaded structures using a modal superposition of stress intensity factors, Eng. Fract. Mech. 93
536 (2012) 75–91. doi:http://dx.doi.org/10.1016/j.engfracmech.2012.06.009.

- 537 [21] C. Albuquerque, A.L.L. Silva, A.M.P. de Jesus, R. Calçada, An efficient methodology for
538 fatigue damage assessment of bridge details using modal superposition of stress intensity
539 factors, *Int. J. Fatigue*. 81 (2015) 61–77.
540 doi:<http://dx.doi.org/10.1016/j.ijfatigue.2015.07.002>.
- 541 [22] K. Kiss, L. Dunai, Stress history generation for truss bridges using multi-level models,
542 *Comput. Struct.* 78 (2000) 329–339. doi:10.1016/s0045-7949(00)00079-1.
- 543 [23] K. Kiss, L. Dunai, Fracture mechanics based fatigue analysis of steel bridge decks by two-
544 level cracked models, *Comput. Struct.* 80 (2002) 2321–2331. doi:10.1016/s0045-
545 7949(02)00254-7.
- 546 [24] H. Zhou, G. Shi, Y. Wang, H. Chen, G. De Roeck, Fatigue evaluation of a composite railway
547 bridge based on fracture mechanics through global-local dynamic analysis, *J. Constr. Steel*
548 *Res.* 122 (2016). doi:10.1016/j.jcsr.2016.01.014.
- 549 [25] Z.X. Li, T.Q. Zhou, T.H.T. Chan, Y. Yu, Multi-scale numerical analysis on dynamic
550 response and local damage in long-span bridges, *Eng. Struct.* 29 (2007) 1507–1524.
551 doi:<http://dx.doi.org/10.1016/j.engstruct.2006.08.004>.
- 552 [26] R.W. Clough, J. Penzien, *Dynamics of structures*, McGraw-Hill, 1975.
- 553 [27] ANSYS® Academic Research, Release 17.1, 2017.
- 554 [28] ANSYS® Academic Research, Release 17.1, *Element Reference, Coupled Field Analysis*
555 *Guide*, ANSYS, Inc., 2017.
- 556 [29] A.M.P. de Jesus, R. Matos, B.F.C. Fontoura, C. Rebelo, L. Simões da Silva, M. Veljkovic, A
557 comparison of the fatigue behavior between S355 and S690 steel grades, *J. Constr. Steel Res.*
558 79 (2012) 140–150. doi:<http://dx.doi.org/10.1016/j.jcsr.2012.07.021>.
- 559 [30] L.R.T. Melo, *Estudo de Efeitos Dinâmicos de Pontes Ferroviárias considerando Interação*
560 *Veículo-Estrutura*, Phd Thesis, Universidade de São Paulo, 2016.
- 561 [31] A.L.L. Silva, *Fatigue behavior of an ancient bridge material under complex loads*, Master

- 562 Thesis, Trás-os-Montes and Alto Douro University, 2009.
- 563 [32] ANSYS® Academic Research, Release 17.1, Theory Reference, Coupled Field Analysis
- 564 Guide, ANSYS, Inc., 2017.
- 565